Inorg. Chem. **2008**, *47*, 3173−3181

Inorganic Chemistry
Article

Influence of Volatile Chlorides on the Molten Salt Synthesis of Ternary Oxide Nanorods and Nanoparticles

Per Martin Rørvik,[†] Tone Lyngdal,[†] Ragnhild Sæterli,[‡] Antonius T. J. van Helvoort,[‡] Randi Holmestad,[‡] Tor Grande,[†] and Mari-Ann Einarsrud*,[†]

Department of Materials Science and Engineering and Department of Physics, Norwegian University of Science and Technology, 7491 Trondheim, Norway

Received November 9, 2007

A molten salt synthesis route, previously reported to yield $BaTiO_3$, $PbTiO_3$, and $Na_2Ti_6O_{13}$ nanorods, has been re-examined to elucidate the role of volatile chlorides. A precursor mixture containing barium (or lead) and titanium was annealed in the presence of NaCl at 760 or 820 °C. The main products were respectively isometric nanocrystalline $BaTiO_3$ and $PbTiO_3$. Nanorods were also detected, but electron diffraction revealed that the composition of the nanorods was respectively $BaTi_2O_5$/$BaTi_5O_{11}$ and $Na_2Ti_6O_{13}$ for the two different systems, in contradiction to the previous studies. It was shown that NaCl reacted with BaO (PbO) resulting in loss of volatile $BaCl_2$ ($PbCl_2$) and formation and preferential growth of titanium oxide-rich nanorods instead of the target phase $BaTiO_3$ (or $PbTiO_3$). The molten salt synthesis route may therefore not necessarily yield nanorods of the target ternary oxide as reported previously. In addition, the importance of NaCl(g) for the growth of nanorods below the melting point of NaCl was demonstrated in a special experimental setup, where NaCl and the precursors were physically separated.

Introduction

The synthesis of nanoscale structures has attracted extensive attention in the past decade as a result of their novel size-dependent properties. Intense experimental efforts have been made to prepare nanoparticles, ultrathin films, nanorods, and nanotubes, as well as three-dimensional arrays of nanostructures. Of these, one-dimensional structures such as nanorods and nanotubes are the smallest dimension structures that can be used for the efficient transport of electrons and optical excitations and are thus expected to be critical to the function and integration of components at the nanoscale.[1] The synthesis of nanorods and nanowires has mainly been directed toward metallic, semiconductor, and binary oxide materials,[2–4] but syntheses of complex ternary oxide materials is now rapidly emerging.[5]

The molten salt synthesis is a relatively simple method to prepare ceramic powders, in which a molten salt is used as a reaction medium for reactant dissolution and precipitation. The features of this synthesis method are related to the surface and interface energies between the constituents and the salt, resulting in a tendency to minimize the energies by forming a specific morphology.[6] The powder morphology and characteristics are affected by the preparation conditions, the type of salt, the precursor composition, the initial particle size, and the solubilities of the constituents in the salt.[6] Because the molten salt synthesis method uses multiple source precursors, it is a very attractive method for the commercialization of production of complex oxides with nanosized structure as this simplifies the synthesis.

A molten salt synthesis route to produce oxide nanorods, involving a nonionic surfactant and sodium chloride as the

* To whom correspondence should be addressed. E-mail: mari-ann.einarsrud@material.ntnu.no. Phone: +4773594002.
[†] Department of Materials Science and Engineering.
[‡] Department of Physics.

(1) Hu, J.; Odom, T. W.; Lieber, C. M. *Acc. Chem. Res.* **1999**, *32*, 435–445.
(2) Xia, Y.; Yang, P.; Sun, Y.; Wu, Y.; Mayers, B.; Gates, B.; Yin, Y.; Kim, F.; Yan, H. *Adv. Mater.* **2003**, *15*, 353–389.
(3) Rao, C. N. R.; Deepak, F. L.; Gundiah, G.; Govindaraj, A. *Prog. Solid State Chem.* **2003**, *31*, 5–147.
(4) Law, M.; Goldberger, J.; Yang, P. *Annu. Rev. Mater. Res.* **2004**, *34*, 83–122.
(5) Mao, Y.; Park, T.-J.; Wong, S. S. *Chem. Commun.* **2005**, 5721–5735.
(6) Yoon, K. H.; Cho, Y. S.; Kang, D. H. *J. Mater. Sci.* **1998**, *33*, 2977–2984.
(7) Mao, Y.; Banerjee, S.; Wong, S. S. *J. Am. Chem. Soc.* **2003**, *125*, 15718–15719.
(8) Wang, W.; Xu, C.; Wang, X.; Liu, Y.; Zhan, Y.; Zheng, C.; Song, F.; Wang, G. *J. Mater. Chem.* **2002**, *12*, 1922–1925.
(9) Wang, W.; Xu, C.; Wang, G.; Liu, Y.; Zheng, C. *Adv. Mater.* **2002**, *14*, 837–840.

10.1021/ic702207a CCC: $40.75
Published on Web 02/29/2008

salt, has been described by several authors.[7–13] Nanorods of both binary oxides such as SnO_2,[8] Mn_3O_4,[9] Co_3O_4,[10] and CuO[11] and ternary oxides such as $BaTiO_3$,[7] $PbTiO_3$,[12] $Na_2Ti_6O_{13}$, and $KTi_8O_{16.5}$[13] have been synthesized by this method. The described synthesis procedure is essentially the same for all compositions, consisting of the preparation of a precursor mixture with a nonionic surfactant and the annealing of this mixture in a NaCl flux. The contradiction of the studies of Mao et al.[7] and Xu et al.,[13] which despite similar synthesis conditions (precursor, temperature, time) reported different products ($BaTiO_3$ and $Na_2Ti_6O_{13}$ nanorods, respectively), calls for further investigation of the molten salt method. In addition to the molten salt route, several authors[14–17] have described oxide nanorod synthesis with NaCl at temperatures far below the melting point of NaCl ($T_{m,NaCl}$ = 801 °C). For instance, Deng et al.[14] describe the synthesis of $PbTiO_3$ nanorods at 700 °C using a mixture of $PbTiO_3$ nanoparticles, a nonionic surfactant and NaCl. Their method is strictly speaking not a molten salt method, but the salt was necessary to make nanorods.[14] Also, a significant vapor pressure of NaCl(g) might be important for the growth mechanism in the absence of molten salts.

In this study we describe a molten salt synthesis at 820 °C with barium (or lead) and titanium precursors, similar to the procedure reported by others.[7,13] With the barium precursor, a small fraction of $BaTi_2O_5$ nanorods were formed in addition to isometric $BaTiO_3$ nanoparticles. With the lead precursor, $Na_2Ti_6O_{13}$ nanorods and $PbTiO_3$ nanoparticles were formed. These findings are discussed in relation to the volatility of $BaCl_2$ and $PbCl_2$. In a modified synthesis procedure at 760 °C with separation of salt and precursors, we obtained similar results, which demonstrates that NaCl(g) affects the synthesis already below the melting point of NaCl.

Experimental Section

Synthesis. We first conducted the standard synthesis procedure[7,13] which is as follows. Barium oxalate (British Drug House Ltd., laboratory grade) was mixed with titanium oxide (anatase, Merck, >99%), sodium chloride (SDS France, >99%), and polyoxyethylene(9) nonylphenyl ether (NP-9, Aldrich, Igepal CO-630) in the molar ratio 1:1:20:3. The mixture was ground for 25 min in an agate mortar, sonicated for 5 min, and then placed in a platinum crucible. The surfactant acted as a dispersing agent preventing agglomeration during the precursor mixture preparation. The crucible with contents was heated at 820 ± 2 °C for 3.5 h in a vertical tube furnace (diameter 6 cm) with a heating and cooling rate of 200 °C/h and a continuous flow of synthetic air through the furnace (100 mL/min). The temperature gradient along the crucible was ≤2 °C. The product was collected after cooling to room temperature, washed, centrifugated several times with distilled water until no free chloride ions were detected by a silver nitrate solution, and finally dried at 100 °C for 12 h. Similar experiments were done with lead oxalate (Alfa Aesar, 99.999% metals basis) replacing barium oxalate, and a synthesis time of 24 h was then necessary to react the precursors because of the lower solubility of PbO than of BaO in NaCl.[18]

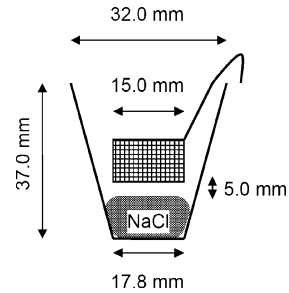

Figure 1. Schematic cross-section of the platinum crucible with the platinum net basket containing the precursor mixture, which was physically separated from the NaCl salt, in the modified synthesis procedure.

A modified synthesis procedure was introduced to investigate the influence of NaCl(g) by physically separating the precursors from the salt. First, the cation precursor mixture was preheated to 300–400 °C for several hours in air to remove the organic constituents (NP-9). The dry precursor mixture was placed into a platinum net basket (diameter 15 mm) with 0.5 mm holes. The net basket was lowered a certain distance into the platinum crucible containing NaCl (3 g, powder with typical cube length 1 mm), carefully securing that there was no contact between the net basket and the NaCl (Figure 1). The distance between the NaCl and the net basket was about 5 mm. The crucible with the net basket was then heat-treated for 24 h, with the same procedure as described above, although at a lower temperature (760 ± 2 °C, except the PT-C synthesis). $BaTiO_3$ and $PbTiO_3$ are formed at 760 °C even without NaCl present, so the only purpose was to observe a possible morphology change induced by NaCl(g). Table 1 gives an overview of the synthesis parameters for the various syntheses. Syntheses with barium are labeled BT; syntheses with lead, PT.

In the PT-B and PT-E syntheses, a Pb−Ti gel precursor was used to investigate the effect of a higher degree of homogeneity of the distributed cations. The Pb−Ti gel was made as previously described by Selbach et al.[19] The dried Pb−Ti-gel was ground to powder in an agate mortar and thereafter calcined at either 400 or 600 °C for 6 h in air to remove the organic constituents prior to use.

Characterization. Thermogravimetric analysis (TGA, Netzsch STA 449C) of the precursor mixture as used in the syntheses BT-A and PT-A was performed using an alumina crucible and a continuous flow of synthetic air (30 mL/min).

The phase composition of the products was studied by X-ray powder diffraction (XRD) using either a Siemens D5005 or a Philips PW 1730/10 diffractometer, both with Cu Kα radiation. A step size of 0.02° and a step time of 2 s (Siemens D5005) or 1 s (Philips PW 1730/10) were used. The products of the net basket syntheses were dispersed onto a silicon low-background specimen holder with ethanol.

The morphology of the products was studied using scanning electron microscopy (SEM, Hitachi S-3400N), field emission

(10) Liu, Y.; Wang, G.; Xu, C.; Wang, W. *Chem. Commun.* **2002**, 1486–1487.
(11) Xu, C.; Liu, Y.; Xu, G.; Wang, G. *Mater. Res. Bull.* **2002**, *37*, 2365–2372.
(12) Cai, Z.; Xing, X.; Yu, R.; Sun, X.; Liu, G. *Inorg. Chem.* **2007**, *46*, 7423–7427.
(13) Xu, C.-Y.; Zhang, Q.; Zhang, H.; Zhen, L.; Tang, J.; Qin, L.-C. *J. Am. Chem. Soc.* **2005**, *127*, 11584–11585.
(14) Deng, Y.; Wang, J. L.; Zhu, K. R.; Zhang, M. S.; Hong, J. M.; Gu, Q. R.; Yin, Z. *Mater. Lett.* **2005**, *59*, 3272–3275.
(15) Li, L.; Wang, W. *Solid State Commun.* **2003**, *127*, 639–643.
(16) Baranov, A. N.; Chang, C. H.; Shlyakhtin, O. A.; Panin, G. N.; Kang, T. W.; Oh, Y.-J. *Nanotechnology* **2004**, *15*, 1613–1619.
(17) Baranov, A. N.; Panin, G. N.; Kang, T. W.; Oh, Y.-J. *Nanotechnology* **2005**, *16*, 1918–1923.
(18) Cherginets, V. L. *Electrochim. Acta* **1997**, *42*, 3619–3627.
(19) Selbach, S. M.; Wang, G.; Einarsrud, M.-A.; Grande, T. *J. Am. Ceram. Soc.* **2007**, *90*, 2649–2652.

Table 1. Selected Synthesis Conditions, Observed Phases, and Rod Morphology for the Different Experiments

label[a]	temperature [°C]	time [h]	method	precursor amount[b] [mmol]	observed phases XRD[c]	observed phases TEM	rod fraction[d] [%]	rod length[e] [μm]	rod diameter[e] [nm]	aspect ratio[e]
BT-A	820	3.5	standard	4.29	$BaTiO_3$ $BaCO_3$ $BaTi_2O_5$	$BaTiO_3$ $BaTi_2O_5$	~20	1–25	50–600	10–60
BT-B	760	24	BaC_2O_4/TiO_2/NP-9 ground/preheated net basket	0.82	$BaTiO_3$		~90[f]	1–5	40–500	4–60
BT-C	760	24	BaC_2O_4/TiO_2/NP-9 ground/preheated net basket	0.13	$BaTiO_3$ $BaTi_5O_{11}$ $BaCl_2$	$BaTiO_3$ $BaTi_5O_{11}$	~20	0.8–7	80–600	3–12
PT-A	820	24	standard	3.0	$PbTiO_3$ TiO_2	$PbTiO_3$ $Na_2Ti_6O_{13}$ TiO_2 $Na_2Ti_9O_{19}$	~20	1–100	50–2000	7–150
PT-B	820	24	calcined gel (600 °C) with NP-9	3.0	$PbTiO_3$ ($Na_2Ti_6O_{13}$)		~10	4–115	60–3000	10–150
PT-C	820	24	PbC_2O_4/TiO_2/NP-9 ground/preheated net basket	0.18	$Na_2Ti_6O_{13}$ $PbTiO_3$ TiO_2		~90	2–70	50–2000	4–120
PT-D	760	24	PbC_2O_4/TiO_2/NP-9 ground/preheated net basket	0.26	$PbTiO_3$		~5	5–18	80–1000	10–80
PT-E	760	24	calcined gel (400 °C) without NP-9 net basket	0.11	$PbTiO_3$ $Na_2Ti_6O_{13}$ TiO_2	$PbTiO_3$ $Na_2Ti_6O_{13}$ TiO_2	~30	1–5	40–500	10–60

[a] Syntheses with barium are labeled BT; syntheses with lead, PT. [b] For the precursor amount for the BT syntheses with the net basket it was assumed that the mixture contained $BaCO_3$ and TiO_2 after preheating, in the PT syntheses only oxides. [c] The phases are listed in order of decreasing intensity. [d] The volume fraction of rods was determined by qualitative evaluation of SEM images. [e] The rod length, rod diameter, and aspect ratio were determined from SEM images. [f] The volume fraction of rods was inhomogeneous. At the very lowest part of the product, the rod fraction was ~90%, while the rest of the product did not contain any rods at all.

scanning electron microscopy (FESEM, Hitachi S-4300SE), and transmission electron microscopy (TEM, PT samples: Philips CM30, BT samples: JEOL JEM-2010). The SEM samples were prepared by sprinkling powder on carbon tape and thereafter coated with gold if necessary. The TEM samples were prepared by dispersing the product in ethanol using an ultrasonic bath and placing a droplet of this dispersion onto a 300 Mesh copper grid coated with a holey amorphous carbon film. The crystallinity of individual particles was studied by selected area electron diffraction (SAED). The element composition of the samples was studied by energy-dispersive X-ray spectroscopy (EDS) in both the SEM and the TEM.

FactSage Thermodynamic Calculations. The Equilib program in the thermochemical software and database package FactSage 5.0 (Thermfact 1976–2001) was used to calculate the equilibrium partial pressures of gases and molar amounts of condensed compounds at various temperatures during the synthesis. Lead oxalate, anatase, and sodium chloride were used as condensed reactants, and oxygen and nitrogen were used as atmosphere. The molar ratio (1:1:20: 4.6:18.5) and the amount (3 mmol PbC_2O_4) of reactants reflected the synthesis conditions in the closed furnace as used in the PT-A synthesis, only without gas flow through the furnace. The surfactant (NP-9) was not included in the calculations. Thermodynamic calculations for the corresponding barium system could not be analyzed because of lack of thermodynamic data for titanium oxide-rich barium titanates.

Results

TGA and Thermodynamic Calculations. The TGA of the precursor mixture used in syntheses BT-A and PT-A is shown in Figure 2. At 250–400 °C, NP-9 evaporated ($T_{b,NP\text{-}9}$ = 250 °C) or decomposed, and PbC_2O_4 decomposed to PbO. BaC_2O_4 decomposed to $BaCO_3$ at 400–500 °C.[20] The precursor mixture was then relatively stable until around 800 °C when evaporation of NaCl was initiated, although the temperature was far below the boiling point ($T_{b,NaCl}$ = 1465 °C). TGA also demonstrated that PbO evaporated above 1050 °C, and only solid TiO_2 remained in the mixture.

The calculated partial pressures above the precursor mixture using the PT-A synthesis conditions are shown in Figure 3a. It is evident that the partial pressures of NaCl, $(NaCl)_2$, and $PbCl_2$ become relatively high ($p_i > 10^{-5}$ atm) above 700 °C. This explains the evaporation of NaCl above 800 °C observed by TGA, especially as the amount of precursor mixture was relatively small and there was a continuous flow of air through the chamber.

From the thermodynamic calculations of the condensed species (Figure 3b) it is clear that $PbTiO_3$ is the thermodynamically most stable product. However, the formation of various sodium titanates (Na_2TiO_3 and $Na_8Ti_5O_{14}$) was also predicted from these calculations, although in smaller amounts than $PbTiO_3$. On the basis of Figure 3a,b, the increasing amount of solid sodium titanates with increasing temperature can be attributed to the volatility of lead species ($PbCl_2$, PbO), with the consequence of changing the Pb:Ti ratio in the condensed state. This was confirmed experimentally and is described further below.

Locally the conditions during the synthesis can be reducing because of the presence of small carbon residues from the decomposition of NP-9 (or gel in the PT-B and PT-E syntheses). If reducing conditions (i.e., nitrogen atmosphere with CO/CO_2 from oxalate decomposition) were used in the calculations, then $Na_2Ti_6O_{13}$ was the only stable sodium

(20) Chen, F.; Sørensen, O. T.; Meng, G.; Peng, D. *J. Therm. Anal.* **1998**, *53*, 397–410.

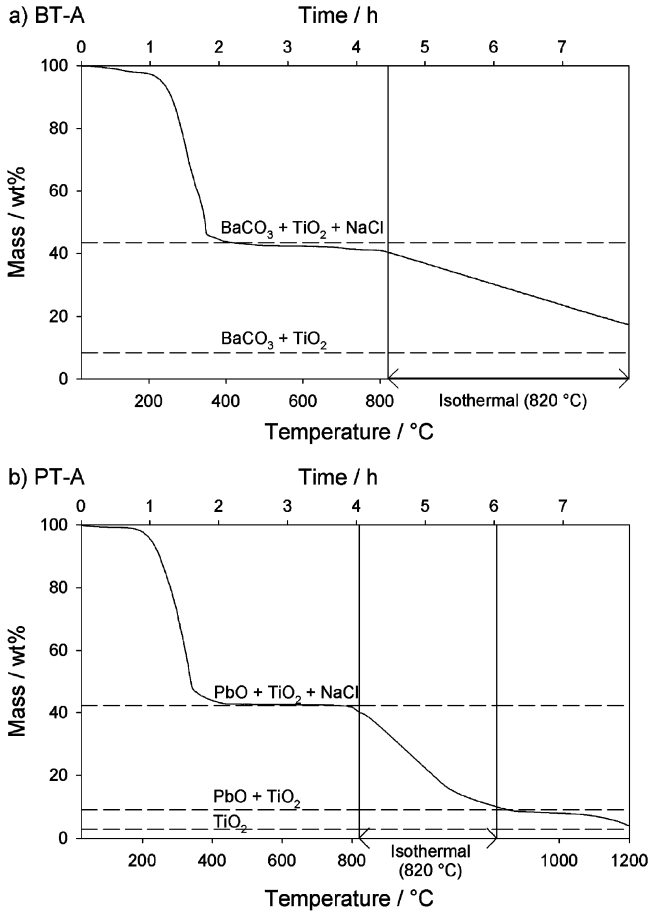

Figure 2. TGA of (a) the BT-A synthesis precursor mixture and (b) the PT-A synthesis precursor mixture. The broken lines represent the theoretical percent of species.

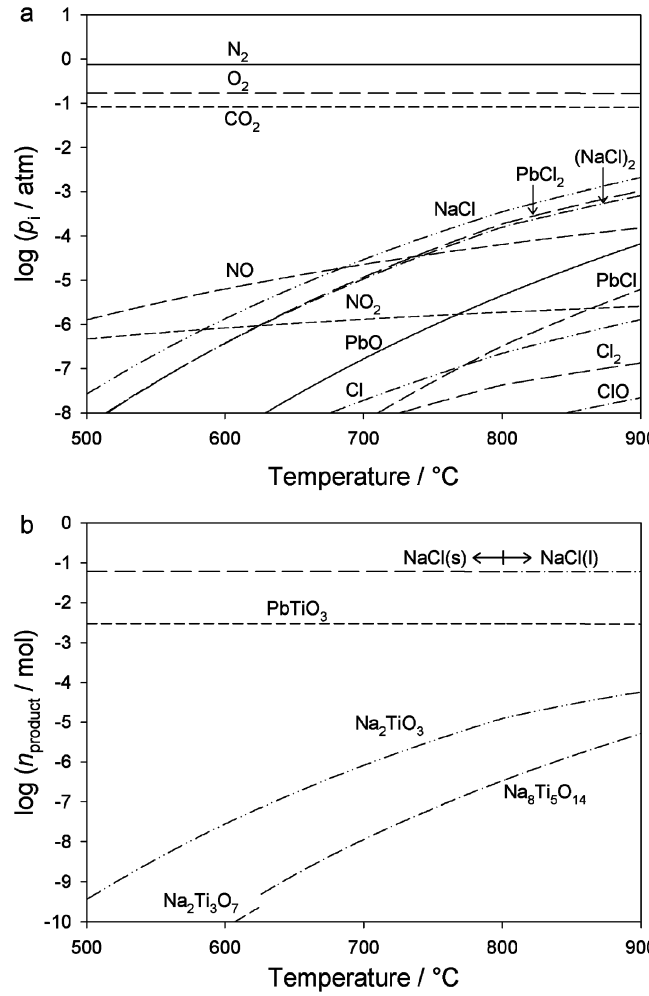

Figure 3. Thermodynamic calculations of (a) partial pressures of gas species (= activity) above the PT-A precursor mixture and (b) amount of condensed species in the PT-A synthesis. The conditions used in the calculations were the same as used in the PT-A synthesis (3 mmol precursor, air atmosphere), only without gas flow through the furnace.

titanate phase (results not shown here). The reducing conditions also resulted in reduction of Pb^{2+} to metallic Pb.

Phase Composition and Morphology of BT Samples. Tetragonal $BaTiO_3$ was the dominant product from the BT syntheses (Figure 4). However, secondary phases ($BaCO_3$ and $BaTi_2O_5$) were present in the BT-A product (Figure 4a), whereas in the BT-B product no secondary phases were observed (Figure 4b). Unwashed BT-C product (Figure 4c) contained a high amount of NaCl, which was removed together with $BaCl_2$ during washing. The X-ray diffractogram of the washed BT-C product (Figure 4d) demonstrates the formation of significant amounts of $BaTi_5O_{11}$ in addition to $BaTiO_3$.

In addition to rods, the BT products consisted also of isometric particles (Figure 5). The qualitative volume fraction of rods was typically ~20% (estimated from SEM images). The diameters of the rods varied from 40 to 600 nm (as measured from SEM and TEM) while the length could be up to 25 μm. The thickness generally increased with increasing length. In general, the rods were straight, but some of the rods were bent (Figure 5c). The rod morphology of syntheses with different conditions is summarized in Table 1.

From the other studies,[7,13] nanorods of either $BaTiO_3$ or $Na_2Ti_6O_{13}$ were expected. However, the TEM examination instead demonstrated the presence of $BaTi_2O_5$ nanorods in the BT-A product (Figure 6) and $BaTi_5O_{11}$ nanorods in the BT-C product (Figure 7). The isometric particles could generally be indexed as tetragonal $BaTiO_3$ (Figure 6b). The existence of $BaTi_2O_5$ and $BaTi_5O_{11}$ is in accordance with the X-ray diffractograms of BT-A and BT-C (Figure 4a,d). None of the examined rods in the BT products could be indexed as $BaTiO_3$ or $Na_2Ti_6O_{13}$. The formation of the titanium oxide-rich barium titanates is in contradiction to the previous studies.

The rods in the BT-B synthesis were not homogeneously distributed, and agglomerates of rods could be observed by SEM. A sample from the bottom part of the BT-B product consisted of several agglomerates with either mainly rods (~90%) or no rods while a sample from the top part of the product consisted only of isometric particles. The rods were thus formed only at the very lowest part of the net basket. In the BT-C product, the rods were more evenly distributed because of the much lower precursor amount used. These observations point to the importance of NaCl(g) for the growth of nanorods.

The BT-B product contained large NaCl cubes even though the starting NaCl powder was physically separated

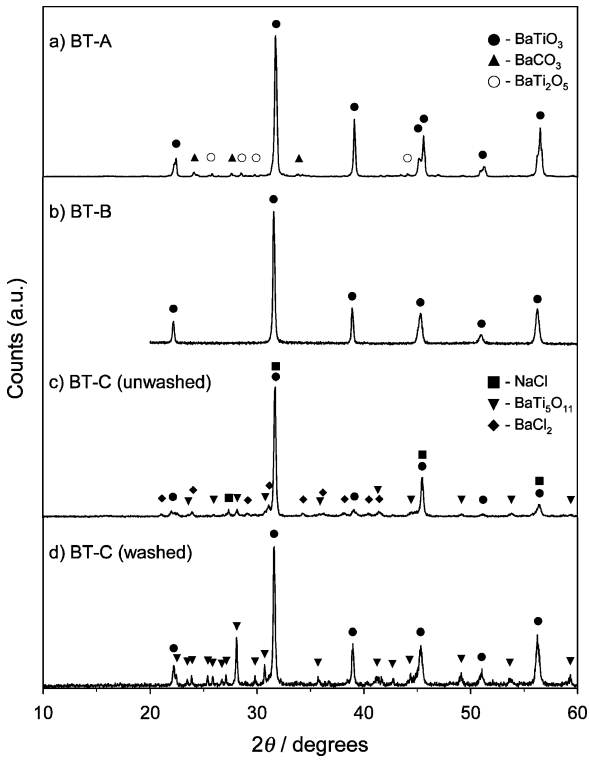

Figure 4. X-ray diffractograms of the BT products: (a) BT-A, (b) BT-B, (c) unwashed BT-C, and (d) washed BT-C. The diffractogram of the BT-B product was not recorded below 20°. The lines are marked according to the Powder Diffraction File (PDF) no.: $BaTiO_3$ (5-626), $BaCO_3$ (45-1471), $BaTi_2O_5$ (34-133), NaCl (5-628), $BaTi_5O_{11}$ (35-805), and $BaCl_2$ (24-94).

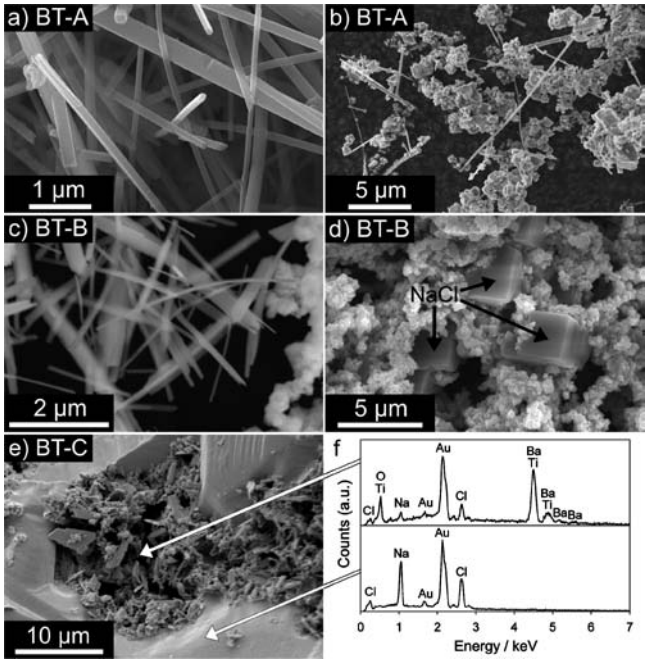

Figure 5. SEM/FESEM images and EDS spectra of the BT products: (a, b) BT-A (the image in b shows the general morphology), (c, d) unwashed BT-B (from the bottom part of the product), and (e, f) unwashed BT-C. The EDS spectra were taken at the indicated spots. The gold peaks in the EDS spectra originate from the gold coating of the SEM sample.

from the precursor mixture (Figure 5d). These cubes were formed by vapor transport of NaCl(g) and consequent condensation (capillary condensation). In the unwashed BT-C product, NaCl actually covered larger areas of the sample

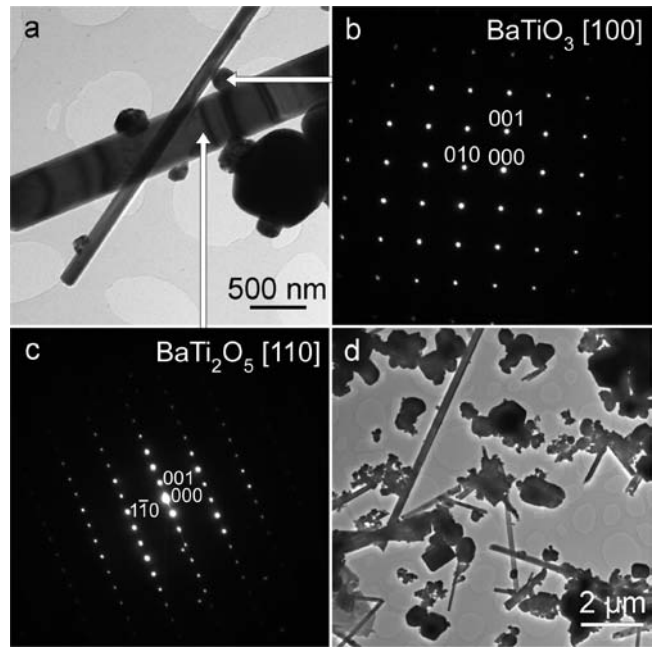

Figure 6. TEM images and SAED patterns of rods and particles in the BT-A product. (a) TEM image. (b) SAED pattern of the particle in a indicated by an arrow. (c) SAED pattern of the rod in a indicated by an arrow. The SAED pattern indicates that the growth direction of the rod is in the [1$\bar{1}$0] direction. (d) Overview TEM image.

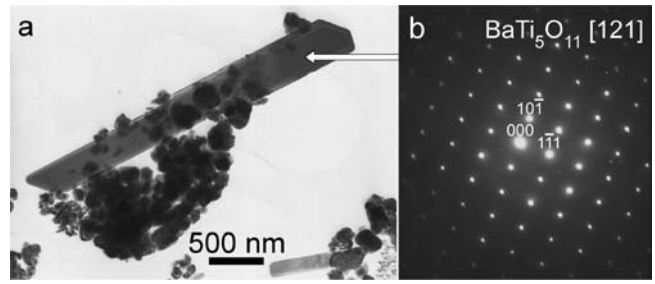

Figure 7. (a) TEM image of rods and particles in the washed BT-C product. (b) SAED pattern of the rod in a indicated by an arrow.

(Figure 5e). The EDS spectra (Figure 5f) clearly show the NaCl content in the smooth areas while the particles in between contained barium and possibly titanium. The exact determination of titanium was difficult because the barium Lα_1 and Lβ_1 peaks (at 4.466 and 4.828 keV, respectively) nearly overlap with the titanium Kα_2, Kα_1, and Kβ_1 peaks (4.505, 4.511, and 4.932 keV, respectively).[21] Barium was easily determined with the Lβ_2 and Lγ_1 peaks (5.157 and 5.531 keV, respectively).[21] The NaCl morphology at the bottom of the crucible did not change markedly during the synthesis at 760 °C.

When the standard synthesis (BT-A) was performed without using NP-9 (either dry mixing or mixing with furfuryl alcohol instead of NP-9), no rods at all were observed in the product.

Phase Composition and Morphology of PT Samples. The PT products consisted mainly of tetragonal $PbTiO_3$, except the PT-C product (Figure 8) which consisted mainly of $Na_2Ti_6O_{13}$ in addition to $PbTiO_3$, anatase, and rutile

(21) Bearden, J. A. *Rev. Mod. Phys.* **1967**, *39*, 78–124.

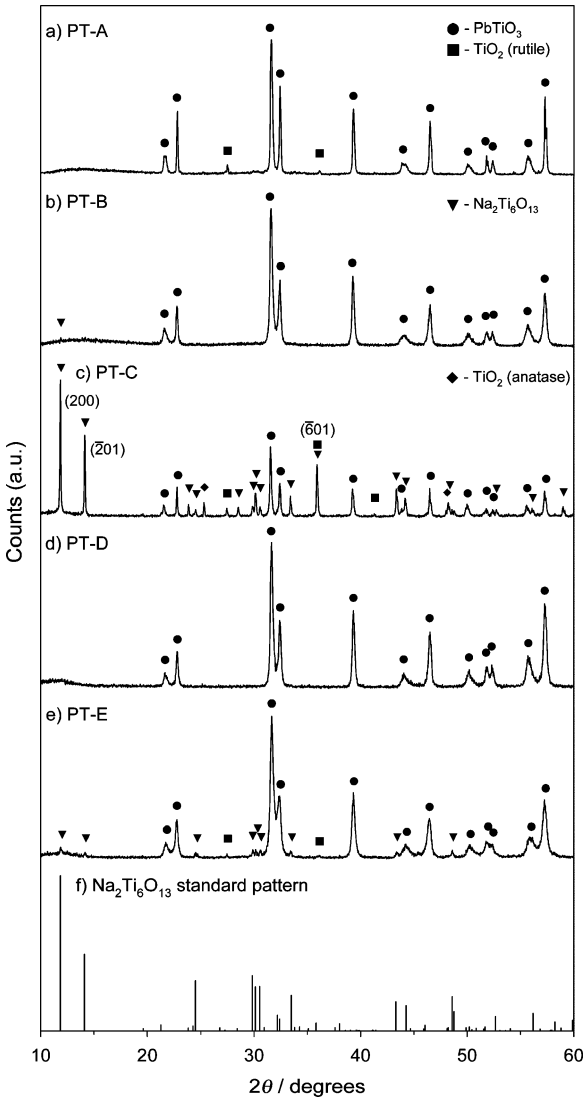

Figure 8. X-ray diffractograms of the PT products: (a) PT-A, (b) PT-B, (c) PT-C ((*hkl*) markings refer to $Na_2Ti_6O_{13}$), (d) PT-D, and (e) PT-E. (f) Standard pattern of $Na_2Ti_6O_{13}$ (PDF no. 73-1398). The amorphous background at 10–20° originates from the sample holder. The lines are marked according to the PDF no.: $PbTiO_3$ (6-452), TiO_2 (rutile 21-1276, and anatase 21-1272), and $Na_2Ti_6O_{13}$ (73-1398).

(Figure 8c). Rutile was transformed from the anatase during heat treatment. Compared with the standard pattern of $Na_2Ti_6O_{13}$ (PDF no. 73-1398, Figure 8f), the diffractogram of the PT-C product had an extra intense line at 35.8°. This has also been described by Teshima et al.,[22,23] who used a NaCl flux at 1100 °C to grow $Na_2Ti_6O_{13}$ whiskers.

The morphology of the PT products was a combination of rods and isometric particles (Figure 9). The qualitative volume fraction of rods varied from ~5% for PT-D to ~90% for PT-C. The diameters of the rods varied from 40 nm to 3 μm (as measured from SEM and TEM) while the length was up to 115 μm. The thickness generally increased with increasing length. The rod morphology of syntheses with different synthesis conditions is summarized in Table 1.

(22) Teshima, K.; Yubuta, K.; Sugiura, S.; Suzuki, T.; Shishido, T.; Oishi, S. *Bull. Chem. Soc. Jpn.* **2006**, *79*, 1725–1728.
(23) Teshima, K.; Sugiura, S.; Yubuta, K.; Suzuki, T.; Endo, M.; Shishido, T.; Oishi, S. *J. Ceram. Soc. Jpn.* **2007**, *115*, 230–232.

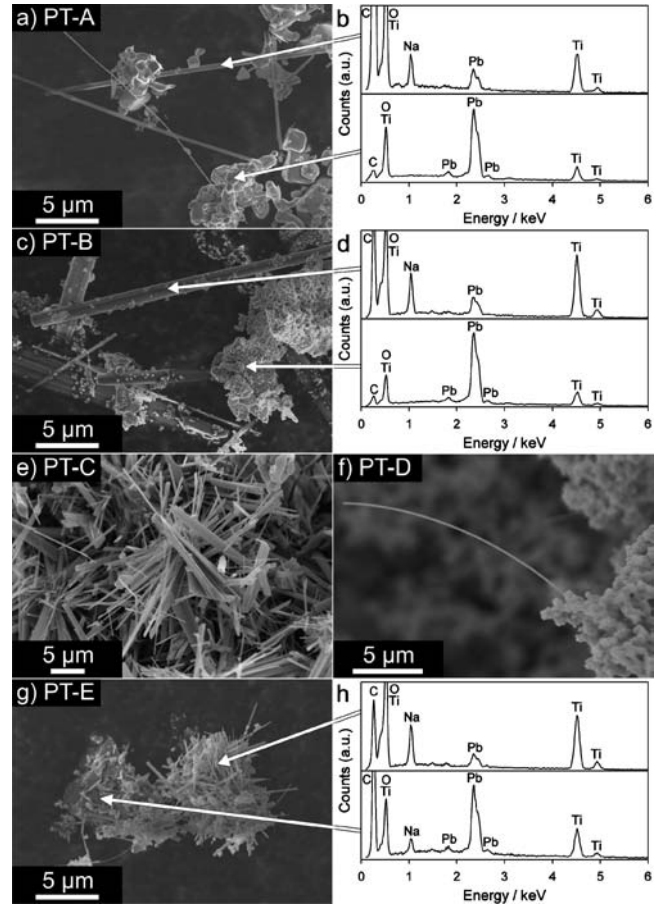

Figure 9. SEM images and EDS spectra of rods and particles in the PT products: (a, b) PT-A, (c, d) PT-B, (e) PT-C, (f) PT-D, and (g, h) PT-E. The EDS spectra were taken at the indicated spots. The carbon peaks in the EDS spectra originate from the carbon tape beneath the rods and particles.

While XRD showed low or no content of sodium titanate for the PT syntheses except PT-C, EDS demonstrated that all the studied rods contained sodium (Figure 9b,d,h) while the isometric particles did not contain Na. The Pb/Ti ratio was correspondingly much lower in the rods than in the isometric particles. If the rods were sodium titanate, the lead peaks might stem from nearby or underlying isometric particles. Lead might also be incorporated into the $Na_2Ti_6O_{13}$ structure, replacing sodium in the tunnels of the crystal structure;[24] however, this is not studied further here.

The TEM examination of the PT-A and PT-E products (Figures 10 and 11, respectively) confirmed the assumptions from the SEM-EDS examination that the rods were composed of sodium titanate. Most of the rods could be indexed as $Na_2Ti_6O_{13}$, a few were indexed as $Na_2Ti_9O_{19}$, and some were not possible to index to any candidate phase considered here. According to the literature,[12,14] $PbTiO_3$ rods were the expected product, both at synthesis below[14] and above[12] $T_{m,NaCl}$, but none of the rods could be indexed as $PbTiO_3$. In contrast, the isometric particles in the products could generally be indexed as $PbTiO_3$ (Figure 11c,d), and, in addition, there was a minor fraction of TiO_2 (rutile) particles. TEM-EDS confirmed the difference in chemical composition

(24) Andersson, S.; Wadsley, A. D. *Acta Crystallogr.* **1962**, *15*, 194–201.

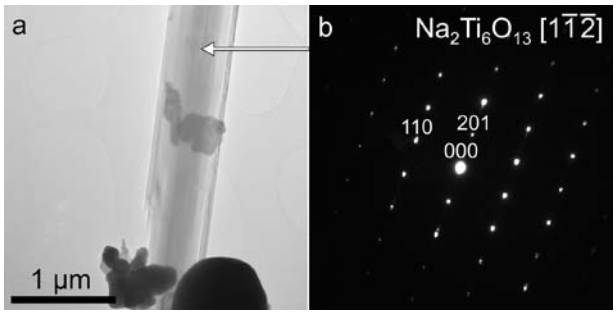

Figure 10. (a) TEM image of a rod and particles in the PT-A product. (b) SAED pattern of the rod in a.

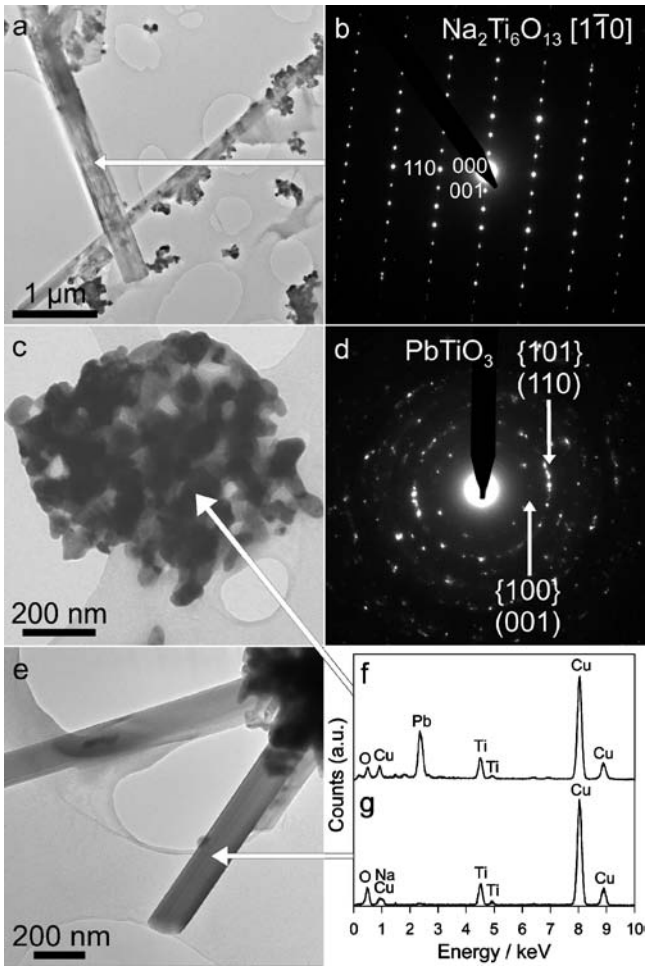

Figure 11. TEM images, SAED patterns, and EDS spectra of rods and particles in the PT-E product. (a) TEM image. (b) SAED pattern of the rod in a indicated by an arrow. (c) TEM image of an agglomerate of $PbTiO_3$ nanoparticles. (d) SAED pattern of the agglomerate in c. (e) TEM image. (f) EDS spectrum of the agglomerate in c. (g) EDS spectrum of the rod in e indicated by an arrow. The copper peaks in the EDS spectra originate from the TEM grid.

between the nanoparticles and nanorods (Figure 11f,g). The spectrum of the agglomerate of nanoparticles in Figure 11c shows a clearly defined lead peak at 2.4 keV, which is absent in the spectrum of the rod in Figure 11e.

Discussion

The BT and PT syntheses did not only yield the expected perovskite phase ($BaTiO_3$ and $PbTiO_3$) with an isometric morphology, but titanium oxide-rich compounds were also formed. None of the examined nanorods had the crystal structure of the perovskite compounds, and the previous studies could not be reproduced.[7,12,14] Neither were $Na_2Ti_6O_{13}$ nanorods produced in the BT-A synthesis, as Xu et al. reported,[13] but $Na_2Ti_6O_{13}$ nanorods were formed in the PT syntheses.

The formation of the isometric perovskite particles can be described by the reaction of the binary constituents:

$$BaCO_3(s) + TiO_2(s) \rightarrow BaTiO_3(s) + CO_2(g) \quad (1)$$

$$PbO(s) + TiO_2(s) \rightarrow PbTiO_3(s) \quad (2)$$

The formation of the titanium oxide-rich compounds suggests an off-set ratio between barium (or lead) and titanium. The thermodynamic calculations (Figure 3) demonstrated the significant vapor pressure of chlorides under the synthesis conditions. The presence of volatile lead chlorides will promote deviation in the Pb/Ti ratio when the amount of cation precursor relative to the salt is small and the synthesis is performed using a gas flow through the furnace. On the basis of this, a proposed formation reaction of $Na_2Ti_6O_{13}$ is

$$2NaCl(g) + PbO(s) + 6TiO_2(s) \rightarrow Na_2Ti_6O_{13}(s) + PbCl_2(g) \quad (3)$$

Diffusion of $PbCl_2(g)$ out of the crucible causes reaction 3 to shift to the right, promoting the formation of $Na_2Ti_6O_{13}$. A similar mechanism is suggested to take place in the BT syntheses, as $BaCl_2$ was detected by XRD in the unwashed product of the BT-C synthesis (Figure 4c). A formation reaction for titanium oxide-rich barium titanates can thus be formulated:

$$2NaCl(g) + 2BaO(s) + xTiO_2 \rightarrow BaTi_xO_{2x+1}(s) + BaCl_2(g/l) + Na_2O(s) \quad (4)$$

The existence of Na_2O in the unwashed BT-C product could not be verified by XRD, and as water will hydrolyze Na_2O, the washing procedure will remove Na_2O in addition to NaCl. As $BaCl_2$ (or possibly barium oxychloride) is less volatile than $PbCl_2$, $BaCl_2$ is more likely to stay in a condensed form, thus not driving the reaction to the right to the same extent as does the more volatile $PbCl_2$. But local evaporation/condensation of $BaCl_2$ can be a driving force for reaction 4. In addition, unreacted $BaCO_3$, which was detected in small amounts in the X-ray diffractogram of BT-A (Figure 4a), will contribute to Ba-deficiency in the product. Xu et al.[13] reported that the use of barium oxalate in the synthesis mixture increased the yield of $Na_2Ti_6O_{13}$ nanowires, indicating a mechanism similar to reaction 3 and supporting the idea that titanium oxide-excess is caused by chloride volatility.

In addition to the $BaCl_2/PbCl_2$ volatility, NaCl(g) was shown to be vital in the nanorod growth in the net basket syntheses conducted below $T_{m,NaCl}$. From reactions 3 and 4, NaCl(g) is a necessary constituent for the formation of $Na_2Ti_6O_{13}$ and $BaTi_xO_{2x+1}$. In fact, when syntheses were conducted without NaCl present, no rods at all were produced, not even in the BT syntheses. Mao et al.[7] and

Deng et al.[14] have also described this phenomenon. $Na_2Ti_6O_{13}$ will not be formed in absence of the salt, and we propose that the salt also has a major influence in the formation of $BaTi_xO_{2x+1}$ rods. This was especially shown in the BT-B synthesis where rods formed only at the bottom of the precursor powder (located more closely to the salt) because of a relatively large amount of precursor mixture in the net basket, reducing the influence of NaCl(g) at the top of the basket. In the PT syntheses with the gel precursor, $PbTiO_3$ is easily formed at 760 °C, even without NaCl present.[19] PT-D and PT-E show that when NaCl(g) is present, some of the precursor will react with NaCl and form $Na_2Ti_6O_{13}$ rods, according to reaction 3. Because the fraction of rods decreases when more precursor mixture is used (see Table 1), very few rods were produced in the PT-D synthesis, and the $Na_2Ti_6O_{13}$ phase could therefore not be detected by XRD. We propose that the volatility of NaCl is important also in similar studies on the formation of nanorods by a NaCl-assisted method below $T_{m,NaCl}$.[14–17] However, in those investigations the salt was mixed with the precursor, so the diffusion distance was much less than in our salt-separated syntheses; the effect of NaCl volatility was thus not easy to detect. The influence of NaCl(g) on the nanorod growth mechanism is uncertain, but NaCl(g) might diffuse to favorable places and form a metastable liquid, which facilitates the growth of nanorods. The metastable liquid may be stabilized either by formation of a microeutectic[17] or by capillary condensation between small precursor particles.

Although a significant amount of $Na_2Ti_6O_{13}$ rods was formed in the PT-A synthesis, the X-ray diffractogram does not show the nanorod phase (Figure 8a). For the BT-B and PT-D syntheses this can be attributed to the low rod volume fraction in the products. But as both EDS (Figure 9b) and SAED (Figure 10b) have confirmed that the rods in the PT-A product were $Na_2Ti_6O_{13}$ instead of $PbTiO_3$, and the rod volume fraction was estimated to 20% (Table 1), the absence of $Na_2Ti_6O_{13}$ diffraction lines is noteworthy. Some possible explanations are overestimation of the nanorod fraction, the lower density of $Na_2Ti_6O_{13}$ compared with that of $PbTiO_3$, and preferential alignment of nanorods during XRD sample preparation leading to reduced intensity. Teshima et al. have observed a difference in the X-ray diffractogram between aligned and pulverized $Na_2Ti_6O_{13}$ whiskers prepared from a NaCl melt; however, the main lines of the standard pattern at 2θ values below 15° were present in both samples.[23]

The XRD results shown here can be misleading if other characterization methods which can characterize individual rods and particles, such as EDS and SAED, are not used. For instance, both Deng et al.[14] and Cai et al.[12] claim to have produced pure $PbTiO_3$ nanorods by a similar method as described here, using NP-9 as an additive, but their X-ray diffractograms only go down to 20°, excluding the main lines of $Na_2Ti_6O_{13}$. In addition, both have low-intensity lines at 24°, 30°, and 33°. This could be regarded as background noise; however, it corresponds to the $Na_2Ti_6O_{13}$ standard pattern (Figure 8f) and the diffractogram of the PT-E product (Figure 8e). The (1 0 1)/(1 1 0) lines in the diffractogram of Deng et al. are not split,[14] indicating crystallites that are much smaller than the 50–80 nm diameter of the nanorods,[25] assuming that the nanorods are single-crystalline as found here. Neither Deng et al. or Cai et al. have used EDS to characterize individual rods. The SAED pattern of Deng et al. is unindexed while that of Cai et al. is misindexed as the indicated zone axis ([0 $\bar{1}$ 2]) has a totally different pattern. Moreover, neither Deng et al. nor Cai et al. have described the rod fraction in their products, and we suggest that they also may have produced $Na_2Ti_6O_{13}$ nanorods instead of $PbTiO_3$ nanorods.

In their $BaTiO_3$ synthesis, Mao et al.[7] reported that the product contained relatively few (isometric) particles, and their EDS examination showed no sodium content in a single nanorod. However, their X-ray diffractogram only goes down to 20° and contains some secondary phases at 27–29°. Their SAED pattern is likely to be misindexed as two identical reflections are listed. Because no sodium was detected by EDS, it is unlikely that they produced $Na_2Ti_6O_{13}$ nanorods, as Xu et al.[13] did with the same method, but the nanorods may be a $BaTi_xO_{2x+1}$ phase as described in this work. The detailed SAED pattern examination of the $Na_2Ti_6O_{13}$ nanorods by Xu et al. is convincing, but it is difficult to explain the different outcome when the same method has been used. However, the influence of volatile chlorides on the synthesis makes the gas flow and gas flow patterns important parameters, which in turn depend on the size and design of the furnace and the crucible. The amount of precursor used in the synthesis is also essential. This essential information is often not described in detail in the literature which makes reproducibility very difficult.

Although no $BaTiO_3$ or $PbTiO_3$ nanorods were detected by SAED in this work, such perovskite nanorods may exist in the products as only a small fraction of the produced nanorods were studied separately by TEM. Our main point is that the molten salt method clearly produces nonperovskite nanorods, so the synthesis method is not ideal for the synthesis of pseudocubic perovskite nanorods. Instead, it seems to be best suited for the synthesis of compounds with highly anisometric crystal structures such as $Na_2Ti_6O_{13}$ because such compounds often more easily form anisometric shapes than compounds with isometric crystal structure.[2] However, to prepare nanorods of compounds with cubic or pseudocubic crystal structure by molten salt synthesis, a possible method is to use a rod-shaped reactant which has a low solubility in the salt. For the systems described here, a rod-shaped TiO_2 precursor can be used as TiO_2 has very low solubility in alkali chlorides.[26] Then the more soluble reactant, such as BaO or PbO,[18,27] can dissolve into the salt and diffuse onto the surface of the less soluble reactant and react there to form the product phase. This has in fact been demonstrated by Cai et al.[12] in another part of their work, using a slightly different synthesis procedure than the one described so far. They show that rod-shaped $PbTiO_3$ is

(25) Erdem, E.; Semmelhack, H.-C.; Böttcher, R.; Rumpf, H.; Banys, J.; Matthes, A.; Gläsel, H.-J.; Hirsch, D.; Hartmann, E. *J. Phys.: Condens. Matter* **2006**, *18*, 3861–3874.
(26) Anikin, I. N.; Naumova, I. I.; Rumyantseva, G. V. *Sov. Phys. Crystallogr.* **1965**, *10*, 172–177.
(27) Packter, A. *Krist. Tech.* **1980**, *15*, 413–420.

formed if the TiO_2 reactant is rod-shaped, but isometric $PbTiO_3$ is formed if the TiO_2 reactant is isometric. This method is therefore a more general approach, which can be used to make nanorods of other ternary oxides, if the appropriate rod-shaped reactant with low solubility in the salt is used, combined with a reactant with a higher solubility.

The nanorod compounds which have been synthesized in this work have several interesting properties, and the nanorods could be of use in a variety of applications if the nanorods can be separated from the nanoparticles or the synthesis optimized for nanorod output. $Na_2Ti_6O_{13}$ has, for instance, been used in an oxygen electrode for a potentiometric CO_2 sensor[28] and as a photocatalyst combined with Ru for the decomposition of water.[29] $BaTi_2O_5$ is a high-T_C ferroelectric,[30] and $BaTi_5O_{11}$ is an attractive candidate for use in resonator devices as the material should have a temperature coefficient of dielectric constant close to zero.[31] The rods can also be used in templated grain-growth of ceramics[32] as well as in composites.

Conclusions

The molten salt method described here is a relatively simple synthesis route for production of single-crystalline nanoparticles and nanorods. The main products were isometric nanocrystalline $BaTiO_3$ and $PbTiO_3$ particles for the two systems studied, but nanorods were also detected. It was demonstrated that the stochiometry of the nanorods was difficult to control because of the formation and volatility of $BaCl_2$ and $PbCl_2$, which resulted in formation of nanorods of titanium oxide-rich compounds rather than the desired perovskites $BaTiO_3$ and $PbTiO_3$. By a salt-assisted method conducted below the melting point of the salt, volatile NaCl was shown to be vital for the growth of nanorods. The experimental results presented here suggest that molten salt synthesis is best suited for the synthesis of nanorods of compounds with highly anisometric crystal structures.

Acknowledgment. The authors thank Yingda Yu for assistance in the TEM work on the BT syntheses products. This work was financially supported by The Strategic Area of Materials at the Norwegian University of Science and Technology and the Research Council of Norway (NANOMAT, under Grant 158518/431, and SUP, under Grant 140553/I30).

IC702207A

(28) Holzinger, M.; Maier, J.; Sitte, W. *Solid State Ionics* **1996**, *86–88*, 1055–1062.
(29) Inoue, Y.; Kubokawa, T.; Sato, K. *J. Phys. Chem.* **1991**, *95*, 4059–4063.
(30) Akishige, Y.; Fukano, K.; Shigematsu, H. *J. Electroceram.* **2004**, *13*, 561–565.
(31) Davies, P. K.; Roth, R. S. *J. Solid State Chem.* **1987**, *71*, 503–512.
(32) Messing, G. L.; Trolier-McKinstry, S.; Sabolsky, E. M.; Duran, C.; Kwon, S.; Brahmaroutu, B.; Park, P.; Yilmaz, H.; Rehrig, P. W.; Eitel, K. B.; Suvaci, E.; Seabough, M.; Oh, K. S. *Crit. Rev. Solid State* **2004**, *29*, 45–96.